International Journal on Semantic Web and Information Systems
Volume 19 • Issue 1

Neuro-Based Consensus Seeking for Nonlinear Uncertainty Multi-Agent Systems Constrained by Dead-Zone Input

Zhenhua Qin, School of Modern Information Technology, Zhejiang Institute of Mechanical and Electrical Engineering, China*

Rongjun Gai, Zhejiang Branch of China Mobile Group Design Institute Co., Ltd., China

ABSTRACT

The topic about consensus target track seeking for high-order nonlinear multi-agent systems (MASs) with unmodeled dynamics, dynamic disturbances, and dead-zone input is considered in the paper. Using the strong nonlinear map characteristic of radial basis function neural networks (RBFNNs), the complex functions arising from recursive procedure are simplified. Also, inspired by input-to-state practical stability (ISpS), the authors construct a dynamical signal in order to counteract the impact of unmodeled dynamics and dynamic disturbances. The bounded inequality expression has been applied to tackle the unknown input of dead zone. Based on this, consensus control protocol suitable for nonlinear constraints has been constructed by using the recursive backstepping technique and adaptive neural network method. Theoretical analysis indicates not only the uniform boundary of all signals in the closed-loop under the neuro-based consensus controller, but uniform ultimate convergence of consensus tracking errors. The final simulations also confirmed the correctness of the theoretical analysis.

KEYWORDS:

Adaptive Backstepping, Dead-Zone Input, Multi-Agent Systems, Neural Networks, Unmodeled Dynamics

INTRODUCTION

Because of the widespread use of MASs in robot network systems, rotorcraft-based unmanned aerial vehicle (RUAV) systems, flight systems, biochemical processes, jet engines and so on, consensus seeking in complex MASs has been pursued for several decades. Various excellent nonlinear technologies have been applied to controller design for MASs, such as neural network control, adaptive control, robust control and backstepping control. Furthermore, combined with some of these control methods, many considerable achievements have been obtained (Sader et al., 2021; Zhao, Tiao & You, 2022; Liu, Wang & Cai, 2021; Shen, Huo & Saab, 2021; Xiao & Dong, 2021). The authors proposed a new neuro-based distributed controller in (Liu, Hu & Li, 2023) to achieve formation cooperation for leader-follower MASs, and a novel Lyapunov function was built to eliminate the influence of state delays. The full-state feedback NNs containment controller was presented for

DOI: 10.4018/IJSWIS.328767
*Corresponding Author

robots with flexible joints while ensuring the security of the robot in (He, Yan & Sun, 2018). The new adaptive fuzzy tracking algorithm was reported in (Sun, Su & Wu, 2020; Zhou & Tang, 2020; Chang, Zhang & Alotaibi, 2020) for nonlinear switched systems. The major characteristics of these distributed control methods are summarized as follows: (i) the nonlinear functions were not required to be known or expressed as linear parametric models because of the strong approximation ability of NNs; (ii) the methods in (Liu, Wang & Cai, 2021; Shen, Huo & Saab, 2021; Xiao, & Dong, 2021) all related to a common issue of `computer explosion' resulting from repeated differentiations in the standard recursive backstepping process; and (iii) the number of adjusted parameters in (Liu, Hu & Li, 2023; He, Yan & Sun, 2018) was too large because it was dependent on the quantities of NN nodes. To overcome the weakness of (ii), the DSC technique was combined with backstepping control to design controllers for multiagent systems (Sun & Ge, 2022; Yang, Zhao & Yuan, 2022), stochastic systems (Chen, Yuan & Yang, 2022), and multi-input multioutput systems (MIMO) (Aghababa & Moradi, 2021). Meanwhile, the problem addressed in (iii) was resolved by taking the norm square's upper bound of the weight vector instead of the vector itself for estimation (Jiang, Su & Niu,2022; Shahvali & Askari, 2022); however, there were still too many parameters to be estimated. On the other hand, notably, unmodelled dynamic and uncertain perturbations widely exist in many industrial plants. Their existence can affect the control performance, even making it unstable. The existence of unmodelled dynamics that may cause system instability was first initiated in (Krstic, Sun & Kokotovic, 1996). Meanwhile, dynamic nonlinear damping design was introduced for linear input unmodelled dynamics to solve global asymptotic stability problems. Furthermore, nonlinear unmodelled dynamics were discussed in (Chang, Zhang, & Alotaibi, 2020), and stochastic cases were discussed in (Li, Li & Chen, 2015; Zhu, Liu & Wen, 2020). A fuzzy control strategy was proposed by constructing an auxiliary dynamical signal aimed at nonlinear systems limited to unmodelled dynamics in (Yang & Wang, 2016). The fuzzy self-adapting control approach has been discussed by integrating the small-gain approach into the backstepping technique focusing on stochastic systems under the constraint of unmodelled dynamics in (Sun, Su &Wu, 2020). Despite these achievements, to date, few studies have focused on tracking systems with existing networked communication, unmodelled dynamics and external perturbations.

Although neuro-based backstepping technologies have made great achievements, most of the results were based on the actuator of each follower running in good condition. However, nonsmooth nonlinear inputs such as hysteresis, input quantization (Chang, Huang & Park, 2020; Qin et al., 2019) and dead zones commonly exist in industrial systems and devices, such as biological optics, electric servomotors and mechanical actuators. Among them, the nonlinear dead-zone input, which means that the actuators cannot perform accurately what the controller requires, has a considerable influence on the system. The system performance may be severely degraded arising from dead-zone existence, which is valuable but most likely to be neglected in control design, especially for distributed control of MASs. The problem of a fuzzy adaptive controller was discussed for a single agent system with nonlinear input in (Li & Tong, 2014; Wu, Sun & Su, 2022), second-order MAS control with dead-zone inputs was considered in (Shen & Shi, 2016) and high-order stochastic MASs in (Hua, Zhang & Guan, 2017). Nevertheless, the systems considered in (Shen & Shi, 2016) and (Hua, Zhang & Guan, 2017) did not involve unmodelled dynamics. Although some useful results have been obtained for dealing with unmodelled dynamics, most research achievements work for a class of simple systems, and those controllers cannot be directly applied to nonlinear systems with existing networked communication. The primary reason for this is that the state of each subsystem is affected by subsystems that communicate with it. In addition, the methods developed in (Shen & Shi, 2016) and (Hua, Zhang & Guan, 2017) are not suitable for the systems described in this paper because they lack robustness of unmodelled dynamics and dynamic disturbances. The controller of each follower depends not only on the information of itself but also on its neighbours. How to address the distributed design for MASs with nonlinear dead-zone input and unmodelled dynamics is the most important motivation of our work, which will be more complex and challenging.

Based on the discussion above, we focus on solving the consensus control law design problem for MASs with unmodelled dynamics, dynamic disturbances and dead-zone input. The contributions of our research are as follows: (i) each dynamic equation is equipped with unmodelled dynamics, dynamic disturbances and dead-zone input, which make systems more general and closer to the actual systems; (ii) the "computer explosion" problem in (Liu, Wang & Cai, 2021; Shen, Huo & Saab, 2021; Xiao & Dong, 2021) caused by the backstepping recursive procedure is removed by combining the dynamic surface control technique with RBFNNs; (iii) only one parameter needs to be estimated for each follower compared with the number of estimated parameters in (Liu, Hu & Li, 2023; Hu, 2012); thus, the computation cost is greatly reduced; and (iv) the proposed controller is robust to unknown dead-zone parameters, unmodelled dynamics and dynamic disturbances.

The remainder of the paper is structured as follows. Section 2 gives the preliminaries. Section 3 states the research question and hypothesis conditions. Section 4 details the design steps of the consensus controller and provides proof of system stabilization. Section 5 validates our proposed algorithm through simulations. Section 6 concludes the paper.

BACKGROUND

In this section, we first formally state the consensus problem of multi-agent systems with unmodelled dynamics, unknown dynamic disturbances and input dead-zone. Then, the authors proceed to discuss the related works in the field.

Problem Statement and Assumptions

Considering an MAS, which contains a single leading node and M following nodes, all the nodes exchange their information through a directed network. The system dynamical equation of the l th agent is expressed as follows:

$$\begin{cases} \dot{r} = \chi(y_l, r, t), \\ \dot{x}_{l,s} = f_{l,s}(\overline{x}_{l,s}) + g_{l,s}(\overline{x}_{l,s})x_{l,s+1} + \Delta_{l,s}(x_l, r, t), \\ \dot{x}_{l,m} = f_{l,m}(\overline{x}_{l,m}) + g_{l,m}(\overline{x}_{l,m})u_l + \Delta_{l,m}(x_l, r, t), \\ y_l = x_{l,1}, \end{cases} \tag{1}$$

where $\overline{x}_{l,s} = [x_{l,1}, x_{l,2}, \cdots, x_{l,m}]^T \in R^m$ with $l = 1, \cdots, M$, $s = 1, 2, \cdots, m$ represents the state vector; $y_l \in R$ is the system output; $q(\cdot)$, $f_{l,s}(\cdot) : R^k \to R$ represent nonlinear unknown continuous functions; $g_{l,s}(\cdot) \neq 0$ is an unknown control gain; $r \in R^{n_r}$ is the unmodelled dynamic; and $\Delta_{l,s}(\cdot)$ is unknown dynamic disturbances. $u_l \in R$ means the dead-zone output represented by

$$u_l = D_l(v_l) = \begin{cases} m_{l,c}(v_l) & v_l \geq b_{l,c} \\ 0 & b_{l,a} < v_l < b_{l,c} \\ m_{l,a}(v_l) & v_l \leq b_{l,a} \end{cases} \tag{2}$$

where v_l indicates the dead-zone input and $b_{l,a} < 0$ and $b_{l,c} > 0$ are unknown.

Remark 1. To the best of our knowledge, high-order MASs without dead-zone input have been discussed in (Shahvali & Askari, 2022; Hasib, Towhid & Islam, 2021), and high-order nonaffine MASs without unmodelled dynamics have been studied in (Pradhan et al., 2022). It is interesting to see that the follower in (1) includes three characteristics: unmodelled dynamics, dynamic disturbances, and dead-zone input. Therefore, the MASs we consider are more general.

In our work, the research target is to explore a suitable tracking law to all the following nodes for system (1) such that it can asymptotically synchronize to the desired output, while it can reach global boundness to all system signals of the closed-loop systems.

To realize the above control strategy, several useful assumed conditions and lemmas need to be prepared.

Assumption 3.1 The nonlinear gain $g_{l,s}(\cdot)$ with known signs satisfies $0 < \underline{g}_l < \left|g_{l,s}(\cdot)\right| \leq \overline{g}_l < \infty$ for $l = 1,2,\cdots,M$. In general, we assume $0 < \underline{g}_l < g_{l,s}(\cdot) \leq \overline{g}_l < \infty$.

Assumption 3.2 (Pradhan et al., 2022) The states $x_{h,1}$ and $x_{d,2}$ are measurable for the h th follower, which satisfy $h \in N_d$, $h = 1,\cdots,M$, $d = 1,\cdots,M$, and $h \neq d$.

Assumption 3.3 (Li & Tong, 2014) If constants $n_{l,s,0}$, $n_{l,s,1}$, $n_{l,q,0}$ and $n_{l,q,1}$ are all positive and satisfy

$$
\begin{aligned}
&0 < n_{l,s,0} \leq n_{l,s}^{'}(w_l) \leq n_{l,s,1}, \quad w_l(t) > b_{l,s} \\
&0 < n_{l,q,0} \leq n_{l,q}^{'}(w_l) \leq n_{l,q,1}, \quad w_l(t) < b_{l,q}
\end{aligned}
$$

where $n_{l,s}^{'}(w_l) = \left(dn_{l,s}(p) / dp\right)\Big|_{p=w_l}$, $n_{l,s}^{'}(w_l) = \left(dn_{l,s}(p) / dp\right)\Big|_{p=w_l}$.

Based on **Assumption 3.3**, by means of the differential intermediate value theorem, the dead-zone input expressed by the piecewise function in (2) can be transformed into a parametric expression as follows:

$$
u_l = K_l^T(t)\Phi_l(t)w_l(t) + \rho_l\left(w_l(t)\right) \tag{3}
$$

where

$$K_l(t) = [K_{l,r}(w_l(t)), K_{l,s}(w_l(t))]^T \text{ , } \Phi_l(t) = [\varphi_{l,r}(t), \varphi_{l,q}(t)]^T \text{ ,}$$

$$
K_{l,s}(w_l) = \begin{cases} 0, & w_l \leq b_{l,q} \\ n_{l,s}^{'}(b_{l,s}), & b_{l,q} < w_l < b_{l,s} \\ n_{l,s}^{'}(\eta_{l,s}(w_l)), & b_{l,s} < w_l < \infty \end{cases} ,
$$

$$
K_{l,q}(w_l) = \begin{cases} n_{l,q}^{'}(\eta_{l,q}(w_l)), & -\infty < w_l < b_{l,q} \\ n_{l,q}^{'}(b_{l,q}), & b_{l,q} < w_l < b_{l,s} \\ 0, & w_l \geq b_{l,s} \end{cases} ,
$$

$$
\varphi_{l,s}(t) = \begin{cases} 1, & w_l > b_{l,q} \\ 0, & w_l \leq b_{l,q} \end{cases} , \ \varphi_{l,q}(t) = \begin{cases} 1, & w_l > b_{l,s} \\ 0, & w_l \leq b_{l,s} \end{cases} ,
$$

$$
\rho_l(w_l) = \begin{cases} -n_{l,s}^{'}(\eta_{l,s}(w_l))b_{l,s}, & w_l \geq b_{l,s} \\ -\left(n_{l,q}^{'}(b_{l,q}) + n_{l,s}^{'}(b_{l,s})\right)w_l, & b_{l,q} < w_l < b_{l,s} \\ -n_{l,q}^{'}(\eta_{l,q}(w_l))b_{l,q} & w_l \leq b_{l,q} \end{cases}
$$

$\eta_{l,q}(w_l) \in (-\infty, b_{l,q})$, $\eta_{l,s}(w_l) \in (b_{l,s}, +\infty)$; $|\rho_l(w_l)| \leq \rho_l^*$, ρ_l^* is an unknown constant.

Remark 2 As mentioned in (Li & Tong, 2014), the unknown dead-zone input can be partitioned into an input term and is similar to the disturbance part. The $K_l^T(t)\Phi_l(t)$ used as the weight coefficient of the input signal is an unknown positive function, which is called the control slope in this paper.

Assumption 3.4 If smooth functions $\lambda_{l,d,1}(\cdot) \geq 0$, $\lambda_{l,d,2}(\cdot) \geq 0$ is monotonically increasing, when $\lambda_{l,d,1}(0) = \lambda_{l,d,2}(0) = 0$ is satisfied, then

$$\left\|\Delta_{l,d}(x_l, z, t)\right\| \leq \lambda_{l,d,1}(\left\|\overline{x}_{l,d}\right\|) + \lambda_{l,d,2}(\left\|z\right\|) \tag{4}$$

Assumption 3.5 For Lyapunov function $V(e)$, class k_∞ function $\alpha_1(\cdot), \alpha_2(\cdot), \gamma_0(\cdot)$ and constants $c > 0$, $d_0 > 0$, if the e-subsystem is exponentially input-to-state practically stable (exp-ISpS), then

$$\alpha_1(\left\|e\right\|) \leq V(e) \leq \alpha_2(\left\|e\right\|) \tag{5}$$

$$\frac{\partial V(e)}{\partial e} q(y_l, e, t) \leq -cV(e) + \gamma_0(\left|x_{l,1}\right|) + d_0 \tag{6}$$

Lemma 3.1 If $y(m,n)$ is a nondecreasing function, there exist $\phi(m) > 0$, $\phi(n) > 0$ then $\left|y(m,n)\right| \leq \phi(m) + \phi(v)$.

Remark 3.2 For the nondecreasing function γ_0, we obtain

$\gamma_0(s) \leq \gamma_0\left(\dfrac{1}{2}s^2 + \dfrac{1}{2}\right) \leq \gamma_0(s^2) + \gamma_0(1)$ by using **Lemma 3.1**, and there exist γ such that $\gamma_0(s) = s\gamma(s)$, we obtain $\gamma_0(s) \leq s^2\gamma(s^2) + \gamma_0(1)$. Then, (6) can be rewritten as

$$\frac{\partial V(e)}{\partial e} q(y_l, e, t) \leq -cV(e) + x_{l,1}^2\gamma\left(x_{l,1}^2\right) + d_0.$$

Lemma 3.2 When the exp-ISpS conditions are met for Lyapunov function $V(e)$, we can always find $T_0 = T_0(c_0, r_0, e_0) \geq 0$, a dynamical function expressed by (Srivastava et al., 2022)

$$\dot{r} = -c_0 r + x^2\gamma(x^2) + d_0 \tag{7}$$

to meet the following expression:

$$V(e) \leq r(t) + B(t_0, t), \forall t \geq t_0 \tag{8}$$

where $B(t_0, T) = 0$, $\forall T \geq t_0 + T_0$ $c_0 \in (0, c)$ and $r_0 = r(t_0) > 0$ are arbitrary constants and $e_0 = e(t_0)$ and t_0 are initial values.

Remark 3.4 According to **Assumption 3.5**, $\alpha_1^{-1}(\cdot)$ is an increasing function because α_1 is a class k_∞ function. From (4) and **Lemma 3.1**,

$$\left\|e\right\| \leq \alpha_1^{-1}\left(r(t) + B(t_0, t)\right) \tag{9}$$

$$\varphi_{l,s,2}\left(\left\|e\right\|\right) \leq \varphi_{l,s,2}\left(\alpha_1^{-1}\left(r(t)+B(t_0,t)\right)\right) \tag{10}$$

Because $\varphi_{l,s,2}{}^{\circ}\alpha_1^{-1}$ is a continuous and positive function, a smooth function $\vartheta_{l,s} \triangleq \varphi_{l,s,2}{}^{\circ}\alpha_1^{-1}$ can be defined to obtain the inequality $\varphi_{l,s,2}(\| e \|) \leq \vartheta_{l,s}(r) + \vartheta_{l,s}\left(B(t_0,t)\right)$.

For $B(t_0,t) > 0$, we can find a constant $\overline{\vartheta}_{l,s}$ that satisfies $\vartheta_{l,s}\left(B(t_0,t)\right) \leq \overline{\vartheta}_{l,s}$. Thus, (4) can be rewritten as

$$\left\|\Delta_{l,s}(x_l,e,t)\right\| \leq \varphi_{l,s}\left(\left\|x_{l,s}\right\|\right) + \vartheta_{l,s}(r) + \overline{\vartheta}_{l,s} \tag{11}$$

Lemma 3.3 For arbitrary variables z and positive ε, the formula

$$0 \leq | z | - z \tanh\left(\frac{z}{\varepsilon}\right) \leq 0.2785\varepsilon \tag{12}$$

is always hold on.

Lemma 3.4 For any variable z and constant $\xi > 0$

$$0 \leq | z | - \frac{z^2}{\sqrt{z^2+\xi^2}} \leq \xi \tag{13}$$

always holds.

Graph Theory (Qin et al., 2019)

The information flow between followers is expressed through a digraph $\mathrm{P} = \{\mathrm{M},\mathrm{H}\}$, in which M represents the nonempty collection of nodes, and the collection of directed edges is expressed as $\mathrm{H} \subset \mathrm{M} \times \mathrm{M}$. Edge $(m,n) \in \mathrm{H}$ directs the communication from m towards node n. The adjacent matrix $\mathcal{B} = [b_{m,n}] \in R^{n\times n}$, $b_{m,m} = 0, b_{m,n} = 1$ if $(n,m) \in \mathrm{H}$, else $a_{i,j} = 0$. Neighbour nodes are defined with sets $\mathcal{N}_m = \{n \,|\, n \in \mathrm{M}, (n,m) \in \mathrm{H}\}$. $\mathcal{N} = \mathcal{C} - \mathcal{B}$ refers to the Laplace matrix, where $\mathcal{C}$ =diag $\{c_1,\cdots,c_N\}$, and $c_i = \sum_{n\in\mathcal{N}_m} b_{mn}$. Define $\mathcal{B}$ =diag $\{b_1,\cdots,b_N\}$ as the leader adjacency matrix; when $b_k = 1$, it represents the communication direction from the leader to the k-th follower; otherwise, $b_k = 0$ means there is no information exchange.

Neural Network

NNs have been widely applied to data processing (Srivastava et al., 2022; Hasib, Towhid & Islam, 2021; Pradhan et al., 2022), pattern classification and recognition (Chiang et al., 2022; Hammad et al., 2021; Yen, Moh & Moh, 2021), and blockchain technology (Nguyen et al., 2021) owing to their strong learning and approximation capability. For an unknown continuous nonlinear function $g(K)$: $g_{nn}(K) = L^T\Phi(K)$, $R^q \to R$, $K \in R^p$ represents the input vector and p denotes the dimension of the NNs. $L = [l_1, l_2, \cdots, l_s]^T \in R^s$ and l_s are the weights of neural networks, and $s > 1$ indicates neural cell numbers. $\Phi(K) = [\varphi_1(K), \varphi_2(K), \cdots, \varphi_s(K)]^T \in R^s$ is the radial basis function with $\varphi_s(K)$

defined by $\varphi_s(K) := \exp\left[-\frac{(K-\rho_s)^T(K-\rho_s)}{\xi_s^2}\right]$, $s = 1,2,\cdots,m$, where $\rho_s = [\rho_{s,1},\rho_{s,2},\cdots,\rho_{s,q}]^T$ refers to the centre of the curve on the x-axis and ξ_s is the width related to the full width at half peak. For an arbitrary expression $g(K)$, there always exists a NN expression $L^{*T}\Phi(K)$ and any $\delta > 0$ to ensure $g(K) = L^{*T}\Phi(K) + \eta(K)$, $\forall K \in R^p$, where L^* indicates the desired weight vector, and it can be expressed as follows:

$$L^* := \arg\min_{L\in R^p}\left\{\sup_{X\in\Omega_X}\left|g(K) - L^T\Phi(K)\right|\right\},\ |\,\eta(K)\,| \le \delta .$$

PROPOSED METHOD

The distributed consensus control design is carried out for system (1) with the backstepping recursive design approach. Then, the analysis of stability is carried out via Lyapunov's direct method. For simplicity, we omit t, $\overline{x}_{l,s}$ and $X_{l,s}$ in the corresponding functions for the following control design procedures.

Neuro-Based Consensus Controller Design

To keep the design simple, we define the unknown positive constant as

$$\theta_l^* = \max\left\{\left\|W_{l,s}^*\right\| / \underline{g}_l, j = 1,2,\cdots,M\right\} \tag{14}$$

where $W_{l,s}^*$ indicates the optimal weight vector of the neural network. Let $\hat{\theta}_l$ be the estimated value of θ_l. $\tilde{\theta}_l = \theta_l - \hat{\theta}_l$ denotes the estimation error. We introduce the following graph-based error surfaces for $l = 1,2,\cdots,M$, $s = 2,\cdots,m$

$$z_{l,1} = \sum_{s\in N_l} a_{l,s}(y_l - y_s) + b_l(y_l - y_r) \tag{15}$$

$$z_{l,s} = x_{l,s} - \pi_{l,s} \tag{16}$$

$$\xi_{l,s} = \pi_{l,s} - \alpha_{l,s-1} \tag{17}$$

Step 1: To take a derivative with respect to $z_{l,1}$ and substitute (1), we can obtain

$$\dot{z}_{l,1} = p_l\left(\overline{f}_{l,1} + g_{l,1}x_{l,2} + \overline{\Delta}_{l,1} - \sum_{k=1}^{m}\frac{a_{l,k}}{p_l}g_{k,1}x_{k,2} - \frac{b_l}{p_l}\dot{y}_r\right) \tag{18}$$

where $\overline{f}_{l,1} = f_{l,1} - \sum_{k\in N_l}\frac{a_{l,k}}{p_k}f_{k,1}$, $\overline{\Delta}_{l,1} = \Delta_{l,1} - \sum_{k\in N_l}\frac{a_{l,k}}{p_k}\Delta_{k,1}$, $p_k = d_k + b_k$.

Consider the Lyapunov candidate function:

$$V_{l,1} = \frac{1}{2p_l} z_{l,1}^2 + \frac{r^2}{2\lambda_0} \tag{19}$$

where $\lambda_0 > 0$, r is a dynamical signal described by (7).

Taking a derivative with $V_{l,1}$ along (18), the following can be obtained

$$\begin{aligned} \dot{V}_{l,1} = z_{l,1} \Bigg(& \bar{f}_{l,1} + g_{l,1} x_{l,2} - \sum_{k=1}^{m} \frac{a_{l,k}}{p_l} g_{k,1} x_{k,2} \\ & + \bar{\Delta}_{k,1} - \frac{b_l}{p_l} \dot{y}_r \Bigg) + \frac{r}{\lambda_0} \dot{r} \end{aligned} \tag{20}$$

By use of Young's inequality and (11), we obtain the following formulas:

$$\frac{r}{\lambda_0} \dot{r} \le -\left(c_0 \lambda_0^{-1} - \lambda_0^{-2}\right) r^2 + \frac{1}{2} z_{l,1}^4 \gamma^2 \left(z_{l,1}^2\right) + \frac{1}{2} d_0^2 \tag{21}$$

$$z_{l,1} \Delta_{l,1} \le z_{l,1}^2 \left(\varphi_{l,1}^2 + \vartheta_{l,1}^2 + \frac{1}{2} \right) + \frac{1}{2} \bar{\vartheta}_{l,1}^2 + \frac{1}{2} \tag{22}$$

$$\begin{aligned} -z_{l,1} \sum_{k \in N_l} \frac{a_{l,k}}{p_l} \Delta_{k,1} \le {} & z_{l,1}^2 \sum_{k \in N_l} \left(\frac{a_{l,k}}{p_l} \right)^2 \left(\varphi_{k,1}^2 + \vartheta_{k,1}^2 + \frac{1}{2} \right) \\ & + \frac{1}{2} \sum_{k \in N_l} \bar{\vartheta}_{k,1}^2 + \frac{N-1}{2} \end{aligned} \tag{23}$$

Substituting (21)-(23) into (20), we obtain

$$\begin{aligned} & \dot{V}_{l,1} \le z_{l,1} \left(g_{l,1} (z_{l,2} + \xi_{l,2} + \alpha_{l,1}) + F_{l,1}(Z_{l,1}) \right) - \frac{1}{2} \bar{g}_l z_{l,1}^2 \\ & -\left(c_0 \lambda_0^{-1} - \lambda_0^{-2}\right) r^2 - \frac{1}{2} z_{l,1}^2 + \frac{1}{2} \bar{\vartheta}_{l,1}^2 + \frac{1}{2} \sum_{k \in N_l} \bar{\vartheta}_{k,1}^2 + \frac{1}{2} d_0^2 + \frac{N}{2} \end{aligned} \tag{24}$$

where

$$\begin{aligned} F_{l,1}(Z_{l,1}) = {} & \bar{f}_{l,1} - \sum_{k=1}^{m} \frac{a_{l,k}}{p_l} g_{k,1} x_{k,2} - \frac{b_l}{p_l} \dot{y}_r + \frac{1}{2} \bar{g}_l z_{l,1} \\ & + z_{l,1} \left(\varphi_{l,1}^2 + \vartheta_{l,1}^2 + \sum_{k \in N_l} \left(\frac{a_{l,k}}{p_l} \right)^2 \left(\varphi_{k,1}^2 + \vartheta_{k,1}^2 + \frac{1}{2} \right) \right) \\ & + z_{j,1} + \frac{1}{2} z_{j,1}^3 \gamma^2 (z_{j,1}^2) \end{aligned} \tag{25}$$

is an unknown nonlinear function with $Z_{l,1} = \left[x_{l,1}, x_{k,1}, x_{k,2}, z_{l,1}, \dot{y}_r, r \right]^T$.

By employing an RBFNN $W_{l,1}^{T}S_{l,1}(Z_{l,1})$ to approach unknown continuous nonlinear expression $F_{l,1}(Z_{l,1})$, we have

$$F_{l,1}(Z_{l,1}) = W_{l,1}^{*T}S_{l,1}(Z_{l,1}) + \delta_{l,1} \tag{26}$$

where $\delta_{l,1}$ represents the error between the approach value and the actual value, and there is an upper bound $|\delta_{l,1}| \le \bar{\delta}_{l,1}$.

To simplify the expression, the parameter $Z_{l,1}$ is omitted from the function expression.

Utilizing Young's inequality and (12), it is further obtained that

$$\begin{aligned} z_{l,1}W_{l,1}^{*T}S_{l,1} &\le |z_{l,1}|\left\|W_{l,1}^{*}\right\|\left\|S_{l,1}\right\| \\ &\le z_{l,1}\theta_{j}\underline{g}_{l}\|S_{l,1}\|\tanh\left(\frac{z_{l,1}\|S_{l,1}\|}{\varepsilon_{l,1}}\right) + \theta_{l}\underline{g}_{l}\bar{\varepsilon}_{l,1} \end{aligned} \tag{27}$$

$$z_{l,1}\delta_{l,1} \le \frac{1}{2}z_{l,1}^{2} + \frac{1}{2}\bar{\delta}_{l,1}^{2} \tag{28}$$

where $\bar{\varepsilon}_{l,1} = 0.2785\varepsilon_{l,1}$.

Formulas (26)-(28) are substituted into (24) to yield

$$\begin{aligned} \dot{V}_{l,1} \le{}& z_{l,1}g_{l,1}\alpha_{l,1} + z_{l,1}\theta_{l}\underline{g}_{l}\left\|S_{l,1}\right\|\tanh\left(\frac{z_{l,1}\left\|S_{l,1}\right\|}{\varepsilon_{l,1}}\right) \\ & -\frac{1}{2}\bar{g}_{l}z_{l,1}^{2} + z_{l,1}g_{l,1}\xi_{l,2} + g_{l,1}z_{l,1}z_{l,2} \\ & + D_{l,1} - \left(c_{0}\lambda_{0}^{-1} - \lambda_{0}^{-2}\right)r^{2} \end{aligned} \tag{29}$$

where $D_{l,1} = \theta_{l}\underline{g}_{l}\bar{\varepsilon}_{l,1} + \frac{1}{2}\bar{\delta}_{l,1}^{2} + \frac{1}{2}\bar{\vartheta}_{l,1}^{2} + \frac{1}{2}\sum_{k\in N_{l}}\bar{\vartheta}_{k,1}^{2} + \frac{N}{2} + \frac{1}{2}d_{0}^{2}$.

Selecting the first virtual control law $\alpha_{l,1}$, which is expressed by

$$\alpha_{l,1} = -k_{l,1}z_{l,1} - \hat{\theta}_{l}\left\|S_{l,1}\right\|\tanh\left(\frac{z_{l,1}\left\|S_{l,1}\right\|}{\varepsilon_{l,1}}\right) \tag{30}$$

where $k_{l,1} > 0$ and $\varepsilon_{l,1} > 0$ are selected control parameters, it is obtained that

$$z_{l,1}g_{l,1}\alpha_{l,1} \le -k_{l,1}\underline{g}_{l}z_{l,1}^{2} - z_{l,1}\hat{\theta}_{l}\underline{g}_{l}\left\|S_{l,1}\right\|\tanh\left(\frac{z_{l,1}\left\|S_{l,1}\right\|}{\varepsilon_{l,1}}\right) \tag{31}$$

Applying Young's inequality, the formula below is achieved through calculation:

$$g_{l,1}z_{l,1}z_{l,2} \leq \frac{1}{2}\overline{g}_l z_{l,1}^2 + \frac{1}{2}\overline{g}_l z_{l,2}^2 \tag{32}$$

Substituting Formulas (31) and (32) into (29) yields

$$\begin{aligned} \dot{V}_{l,1} &\leq -k_{l,1}\underline{g}_l z_{l,1}^2 + z_{l,1}\tilde{\theta}_l \underline{g}_l \left\|S_{l,1}\right\| \tanh\left(\frac{z_{l,1}\left\|S_{l,1}\right\|}{\varepsilon_{l,1}}\right) \\ &+ z_{l,1}g_{l,1}\xi_{l,2} + \frac{1}{2}\overline{g}_l z_{l,2}^2 + D_{l,1} - \left(c_0\lambda_0^{-1} - \lambda_0^{-2}\right)r^2 \end{aligned} \tag{33}$$

To overcome the "explosion of differentiation of the virtual control", we introduce the filtering $\pi_{l,2}$, which is produced by passing through a first-order filter with constant $l_{l,2}$ of virtual control $\alpha_{l,2}$ as

$$l_{l,2}\dot{\pi}_{l,2} + \pi_{l,2} = \alpha_{l,1}, \pi_{l,2}(0) = \alpha_{l,1}(0) \tag{34}$$

Step s $(2 \leq s \leq m-1)$: Following a similar process to the above at each step.

The time derivative of $z_{l,s}$ becomes

$$\dot{z}_{l,s} = f_{l,s} + g_{l,s}x_{l,s+1} + \Delta_{l,s} - \dot{\pi}_{l,s} \tag{35}$$

Choosing the following Lyapunov candidate function

$$V_{l,s} = V_{l,s-1} + \frac{1}{2}z_{l,s}^2 + \frac{1}{2}\xi_{l,s}^2 \tag{36}$$

The differential operator of $V_{l,s}$ along (35) satisfies

$$\begin{aligned} \dot{V}_{l,s} = z_{l,s}&\left(f_{l,s} + g_{l,s}x_{l,s+1} + \Delta_{l,s} - \dot{\pi}_{l,s}\right) \\ &+ \dot{V}_{l,s-1} + \xi_{l,s}\dot{\xi}_{l,s} \end{aligned} \tag{37}$$

Utilizing Young's inequality again and (11), the following expression can be obtained:

$$z_{l,s}\Delta_{l,s} \leq z_{l,s}^2\left(\varphi_{l,s}^2 + \vartheta_{l,s}^2\right) + \frac{1}{2}z_{l,s}^2 + \frac{1}{2}\overline{\vartheta}_{l,s}^2 + \frac{1}{2} \tag{38}$$

Substituting (16), (17) and (38) into (37), we obtain

$$\begin{aligned}\dot{V}_{l,s} &\le z_{l,s}\left(g_{l,s}(z_{l,s+1}+\xi_{l,s+1}+\alpha_{l,s})+F_{l,s}(Z_{l,s})\right)\\ &\quad -\overline{g}_l z_{l,s}^2-\frac{1}{2}z_{l,s}^2+\frac{1}{2}\overline{\vartheta}_{l,s}^2+\xi_{l,s}\dot{\xi}_{l,s}+\dot{V}_{l,s-1}\end{aligned} \tag{39}$$

where

$$F_{l,s}(Z_{l,s})=f_{l,s}+(\overline{g}_l+1)z_{l,s}+z_{l,s}(\varphi_{l,s}^2+\vartheta_{l,s}^2)-\dot{\pi}_{l,s} \tag{40}$$

is a nonlinear function with unknown items and

$$Z_{l,s}=[\overline{x}_{l,s},z_{l,s},\dot{\pi}_{l,s},r]^T.$$

An RBFNN $W_{l,s}^T S_{l,s}(Z_{l,s})$ is applied to approach the uncertain nonlinear function $F_{l,s}(Z_{l,s})$, and we have

$$F_{l,s}(Z_{l,s})=W_{l,s}^{*T}S_{l,s}(Z_{l,s})+\delta_{l,s} \tag{41}$$

where $\delta_{l,s}$ represents the approach error with upper bound $|\delta_{l,s}|\le\overline{\delta}_{l,s}$.

According to Young's inequality and (12), we have that

$$\begin{aligned}z_{l,s}W_{l,s}^{*T}S_{l,s} &\le |z_{l,s}|\left\|W_{l,s}^*\right\|\left\|S_{l,s}\right\|\\ &\le z_{l,s}\theta_l\underline{g}_l\left\|S_{l,s}\right\|\tanh\left(\frac{z_{l,s}\left\|S_{l,s}\right\|}{\varepsilon_{l,s}}\right)+\theta_l\underline{g}_l\overline{\varepsilon}_{l,s}\end{aligned} \tag{42}$$

$$z_{l,s}\delta_{l,s}\le\frac{1}{2}z_{l,s}^2+\frac{1}{2}\overline{\delta}_{l,s}^2 \tag{43}$$

where $\overline{\varepsilon}_{l,s}=0.2785\varepsilon_{l,s}$.

Substituting Formulas (41)-(42) into (39) yields

$$\begin{aligned}&\dot{V}_{l,s}\le z_{l,s}g_{l,s}\alpha_{l,s}+z_{l,s}g_{l,s}\xi_{l,s+1}+g_{l,s}z_{l,s}z_{l,s+1}\\ &-\overline{g}_l z_{l,s}^2+z_{l,s}\theta_l\underline{g}_l\left\|S_{l,s}\right\|\tanh\left(\frac{z_{l,s}\left\|S_{l,s}\right\|}{\varepsilon_{l,s}}\right)\\ &+\theta_j\underline{g}_j\overline{\varepsilon}_{j,k}+\frac{1}{2}\overline{\delta}_{j,k}^2+\frac{1}{2}\overline{\vartheta}_{j,k}^2+\frac{1}{2}+\xi_{j,k}\dot{\xi}_{j,k}+\dot{V}_{j,k-1}\end{aligned} \tag{44}$$

Based on the above, virtual control law $\alpha_{l,s}$ is expressed by the following equation:

$$\alpha_{l,s}=-k_{l,s}z_{l,s}-\hat{\theta}_l\left\|S_{l,s}\right\|\tanh\left(\frac{z_{l,s}\left\|S_{l,s}\right\|}{\varepsilon_{l,s}}\right) \tag{45}$$

where $k_{l,s} > 0$ and $\varepsilon_{l,s} > 0$ are design parameters; then, we obtain

$$\begin{aligned} & z_{l,s} g_{l,s} \alpha_{l,s} \\ & \leq -k_{l,s} \underline{g}_l z_{l,s}^2 - z_{l,s} \hat{\theta}_l \underline{g}_l \left\| S_{l,s} \right\| \tanh\left(\frac{z_{l,s} \left\| S_{l,s} \right\|}{\varepsilon_{l,s}} \right) \end{aligned} \tag{46}$$

Once again, we use Young's inequality, which is obtained

$$g_{l,s} z_{l,s} z_{l,s+1} \leq \frac{1}{2} \overline{g}_l z_{l,s}^2 + \frac{1}{2} \overline{g}_l z_{l,s+1}^2 \tag{47}$$

Plugging Formulas (46) and (47) into (44) yields

$$\begin{aligned} \dot{V}_{l,s} \leq & \tilde{\theta}_j \sum_{s=1}^{m-1} z_{l,s} \underline{g}_j \left\| S_{l,s} \right\| \tanh\left(\frac{z_{l,s} \left\| S_{l,s} \right\|}{\varepsilon_{l,s}} \right) \\ & - \sum_{s=1}^{m-1} k_{l,s} \underline{g}_l z_{l,s}^2 + \sum_{s=1}^{m-1} z_{l,s} g_{l,s} \xi_{l,s+1} + \sum_{s=2}^{m} \xi_{l,s} \dot{\xi}_{l,s} \\ & + \frac{1}{2} \overline{g}_l z_{l,s+1}^2 + D_{l,s} - \left(c_0 \lambda_0^{-1} - \lambda_0^{-2} \right) r^2 \end{aligned} \tag{48}$$

where $D_{l,s} = D_{l,s-1} + \theta_l \underline{g}_l \overline{\varepsilon}_{l,s} + \frac{1}{2} \overline{\delta}_{l,s}^2 + \frac{1}{2} \overline{\vartheta}_{l,s}^2 + \frac{1}{2}$.

Similar to step 1, we introduce virtual filtering $\pi_{l,s+1}$, which is produced by a first-order low-pass filtering of virtual control $\alpha_{l,s}$, and the filter coefficient is constant $l_{l,s+1}$:

$$l_{l,s+1} \dot{\pi}_{l,s+1} + \pi_{l,s+1} = \alpha_{l,s},\ \pi_{l,s+1}(0) = \alpha_{l,s}(0) \tag{49}$$

Step m: We construct the actual control signal v_l in this step. The derivative of $z_{l,m}$ is

$$\dot{z}_{l,m} = g_{l,m} \left(K_l^T(t) \Phi_l(t) v_l + \rho_l(v_l) \right) + F_{l,m}(Z_{l,m}) \tag{50}$$

where

$$\begin{aligned} F_{l,m}(Z_{l,m}) = & \left(1 + \frac{1}{2} \overline{g}_l \right) z_{l,m} - \dot{\pi}_{l,m} \\ & + z_{l,m} \left(\varphi_{l,m}^2 + \vartheta_{l,m}^2 \right) + f_{l,m} \end{aligned} \tag{51}$$

is an unknown nonlinear formula with

$Z_{l,m} = [\bar{x}_{l,m}, z_{l,m}, \dot{\pi}_{l,m}, r]^T$

We define a new auxiliary variable to facilitate design

$$\bar{v}_l = k_{l,m} z_{l,m} + \hat{\theta}_l \left\| S_{l,m} \right\| \tanh\left(\frac{z_{l,m} \left\| S_{l,m} \right\|}{\varepsilon_{l,m}} \right) \tag{52}$$

Based on this, the actual control law v_l and adaptation law for parameters θ_l and β_l are built below:

$$v_l = -\frac{z_{l,m} \hat{\beta}_l^2 \bar{v}_l^2}{\sqrt{z_{l,m}^2 \hat{\beta}_l^2 \bar{v}_l^2 + \xi_l^2}} \tag{53}$$

$$\dot{\hat{\theta}}_l = \sum_{k=1}^{m} \gamma_j z_{l,k} \left\| S_{l,k} \right\| \tanh\left(\frac{z_{l,k} \left\| S_{l,k} \right\|}{\varepsilon_{l,k}} \right) - \mu_l \hat{\theta}_l \tag{54}$$

$$\dot{\hat{\beta}}_l = z_{l,m} \bar{v}_l - \gamma_{\beta_l} \hat{\beta}_l \tag{55}$$

where $\hat{\beta}_l$ is the estimated value of β_l, $\beta_l = 1 / m_{l,0}$ with $m_{l,0} = \min\{m_{l,r,0}, m_{l,k,0}\}$; k_{l,n_l}, $\omega_{l,m}$, γ_l, μ_l and γ_{β_l} are all positive parameters.

Choosing the Lyapunov candidate function

$$V_{l,m} = V_{l,m-1} + \frac{1}{2} z_{l,m}^2 + \frac{1}{2\gamma_l} \tilde{\theta}_l^2 + \frac{1}{2} m_{l,0} \underline{g}_l \tilde{\beta}_l^2 \tag{56}$$

Following a similar procedure from (40) to (43) with $k = m$, to take the derivative of $V_{l,m}$ along (50), we obtain

$$\begin{aligned} \dot{V}_{l,m} \le{} & z_{l,m} g_{l,m} \left(\theta_l \left\| S_{l,m} \right\| \tanh\left(\frac{z_{l,m} \left\| S_{l,m} \right\|}{\varepsilon_{l,m}} \right) \right. \\ & \left. + K_j^T(t) \Phi_j(t) v_j + \bar{v}_j - \bar{v}_j \right) - \frac{1}{\gamma_j} \tilde{\theta}_j \dot{\hat{\theta}}_j + z_{j,m} g_{j,m} \rho_j \\ & - m_{j,0} \underline{g}_j \tilde{\beta}_j \dot{\hat{\beta}}_j + \theta_j \underline{g}_j \bar{\varepsilon}_{j,m} + \frac{1}{2} \bar{\delta}_{j,m}^2 + \frac{1}{2} \bar{\vartheta}_{j,m}^2 + \frac{1}{2} + \dot{V}_{j,m-1} \end{aligned} \tag{57}$$

By using **Lemma 3.4** and $K_l^T(t) \Phi_l(t) \ge m_{l,0}$, the following result holds:

$$\begin{aligned}
& z_{l,m} g_{l,m} K_l^T(t)\Phi_l(t) v_l \\
& = -g_{l,m} K_l^T(t)\Phi_l(t) \frac{z_{l,m}^2 \hat{\beta}_l^2 \overline{v}_l^2}{\sqrt{z_{l,m}^2 \hat{\beta}_l^2 \overline{v}_l^2 + \xi_l^2}} \\
& \leq -m_{l,0} \underline{g}_l \frac{z_{l,m}^2 \hat{\beta}_l^2 \overline{v}_l^2}{\sqrt{z_{l,m}^2 \hat{\beta}_l^2 \overline{v}_l^2 + \xi_l^2}} \\
& \leq \xi_l m_{l,0} \underline{g}_l - z_{l,m} m_{l,0} \underline{g}_l \hat{\beta}_l \overline{v}_l
\end{aligned} \tag{58}$$

By Young's inequality, the two inequality expressions can be obtained as follows:

$$\begin{aligned}
& 2\mu_l \tilde{\theta}_l \hat{\theta}_l \leq -\mu_l \tilde{\theta}_l^2 + \mu_l \theta_l^2 \\
& 2\gamma_{\beta_l} \tilde{\beta}_l \hat{\beta}_l \leq -\gamma_{\beta_l} \tilde{\beta}_l^2 + \gamma_{\beta_l} \beta_l^2
\end{aligned} \tag{59}$$

Plugging Formulas (58) and (59) into (57) yields

$$\begin{aligned}
\dot{V}_{l,m} \leq & -\sum_{k=1}^{m} k_{l,k} \underline{g}_l z_{l,k}^2 - (c_0 \lambda_0^{-1} - \lambda_0^{-2}) r^2 - \frac{\mu_l}{2\gamma_l} \tilde{\theta}_l^2 \\
& - \frac{1}{2} m_{l,0} \underline{g}_l \gamma_{\beta_l} \tilde{\beta}_l^2 + z_{l,m} g_{l,m} \rho_l \\
& + \sum_{k=1}^{m-1} z_{l,k} g_{l,k} \xi_{l,k+1} + \sum_{k=2}^{m} \xi_{l,k} \dot{\xi}_{l,k} + D_{l,m}
\end{aligned} \tag{60}$$

in which $D_{l,m} = D_{l,m-1} + \theta_l \underline{g}_l \overline{\varepsilon}_{l,m} + \frac{1}{2} \overline{\delta}_{l,m}^2 + \frac{1}{2} \overline{\vartheta}_{l,m}^2 + \frac{1}{2}$.

Remark 4.1 In the literature (Shen & Shi, 2016; Hua, Zhang & Guan, 2017), the number of adoption parameters depends on the followers' order or number of neurons, and it is usually higher than one. It is noteworthy that merely one adaptive parameter will be required to be adjusted for all followers in this work; thus, the computational complexity would be greatly reduced by using this proposed control method.

To address the unknown dead zone, **Lemma 3.**4 plays a crucial role. Moreover, the unknown inverse of the control slope is estimated online to offset the negative effect of the unknown dead zone.

Stability Analysis

According to the above analysis and deduction, the major findings are condensed as the following theorem. Then, the analysis of stability for a closed system and uniform boundness are demonstrated, which implies that all the followers can track the reference trajectory consistently.

Theorem 4.1 Considering the MASs characterized by (1), under **Assumptions 3.1-3.5**, each virtual controller (30) and (45), the resulting actual control law (53), and the parameter adaptation laws (54) and (55), the RBFNNs are adopted for all unknown nonlinearities. Then, the MASs can obtain better consensus tracking when the design parameters are properly chosen.

Proof. See Appendix.

NUMERICAL EXAMPLE AND RESULTS ANALYSIS

In the Presence of Dead-Zone Input

In this subsection, we will carry out a simulation to test and demonstrate the validity of the main findings in our work. Taking the nonlinear networked system, for example, which contains one leading node and six following nodes, the relations between agents are represented in Fig. 1. Each subsystem can be described by the second-order dynamics equation.

F1:

$$\begin{cases} \dot{x}_{1,1} = x_{1,1}^2 + x_{1,2} + 0.1\sin(t) \\ \dot{x}_{1,2} = 2x_{1,1} + x_{1,1}x_{1,2} + \left(1 + \dfrac{x_{1,1}^2 x_{1,2}^2}{1 + x_{1,1}^2 x_{1,2}^2}\right) u_1 + 0.1\sin(t) + x_{1,1}z \\ y_1 = x_{1,1} \end{cases} \tag{61}$$

F2:

$$\begin{cases} \dot{x}_{2,1} = x_{2,1}e^{-0.5x_{2,1}} + x_{2,2} \\ \dot{x}_{2,2} = x_{2,1}x_{2,2}^2 + \left(1 + \dfrac{x_{2,1}^2 x_{2,2}^2}{1 + x_{2,1}^2 x_{2,2}^2}\right) u_2 + 0.1z^2\cos(0.2x_{2,2}t) \\ y_2 = x_{2,1} \end{cases} \tag{62}$$

F3:

$$\begin{cases} \dot{x}_{3,1} = 2x_{3,1}\sin(x_{3,1}t) + x_{3,1}x_{3,2} + x_{3,2} \\ \dot{x}_{3,2} = x_{3,1}^2 + x_{3,1}x_{3,2} + (1 + x_{3,1}^2 x_{3,2}^2)u_3 + 2z^2 + \cos(0.5x_{3,1}t) \\ y_3 = x_{3,1} \end{cases} \tag{63}$$

F4:

$$\begin{cases} \dot{x}_{4,1} = x_{4,1}\sin(x_{4,1}t) + x_{4,2} \\ \dot{x}_{4,2} = x_{4,1}x_{4,2} + x_{4,2}^2 + u_4 + 0.1z^2\cos(0.5x_{3,1}t) \\ y_4 = x_{4,1} \end{cases} \tag{64}$$

F5:

$$\begin{cases} \dot{x}_{5,1} = 2x_{5,1}\sin(x_{5,1}t) + x_{5,1}x_{5,2} \\ \dot{x}_{5,2} = x_{5,1}^2 + x_{5,2}\cos(x_{5,1} + x_{5,2}) + x_{5,2}^2 u_5 + 2z^2 \\ y_5 = x_{5,1} \end{cases} \tag{65}$$

F6:

$$\begin{cases} \dot{x}_{6,1} = \sin(x_{6,1}t) + x_{6,1}x_{6,2} \\ \dot{x}_{6,2} = x_{6,1}^2 + x_{6,2}\cos(x_{6,1}) + u_6 + 2z^2 + \cos(0.5x_{6,1}) \\ y_6 = x_{6,1} \end{cases} \tag{66}$$

where $\dot{z} = -z + x_{1,1}^2 + 0.5$.

$$u_l = D_l(v_l) = \begin{cases} \left(1 - 0.3\sin(v_l)\right)(v_l - 2.5) & v_l \geq 2.5 \\ 0, & -1.5 < v_l < 2.5 \\ \left(0.8 - 0.2\cos(v_l)\right)(v_l + 1.5) & v_l \leq -1.5 \end{cases} \tag{67}$$

It is easily obtained that $\underline{g}_l = 1$, $\overline{g}_l = 2$.

Choosing $V(z) = z^2$, we obtain

$$\begin{aligned} \dot{V}_z(z) &= 2z(-z + x_{11}^2 + 0.5) \\ &\leq -2z^2 + \frac{1}{4\beta}(2z)^2 + \beta x_{11}^4 + \frac{\beta}{4} + \frac{z^2}{\beta} \end{aligned} \tag{68}$$

Then, the following expression is obtained by setting parameter $\beta = 2.5$:

$$\dot{V}_z(z) \leq -1.2z^2 + 2.5x_{11}^4 + 0.625 \tag{69}$$

Under **Assumption 3.6**, we can choose $\alpha_1(|z|) = 0.5z^2, \alpha_2(|z|) = 2z^2, \overline{c} = 1 \in (0, 1.2), d_0 = 0.625$ and $\gamma(|x_{11}|) = 2.5x_{11}^4$, and the dynamical signal r is defined as

$$\dot{r} = -r + 2.5x_{1,1}^4 + 0.625 \tag{70}$$

The RBFNN consists of 72 nodes with centres μ_l spread evenly on the interval $[-3, 3]$ with widths $\phi_l = 2$; thus, the continuous nonlinear expressions can be approximated with the help of the RBFNN.

The target trajectory is selected as follows:

$$y_r = \sin(t) \tag{71}$$

The simulation parameters are: $\gamma_{1,1} = \gamma_{1,2} = \gamma_{2,1} = \gamma_{2,2} = \gamma_{3,1} = \gamma_{3,2} = 35$, $\gamma_{4,1} = \gamma_{4,2} = 25$, $\gamma_{5,1} = \gamma_{5,2} = 20$, $\gamma_{6,1} = \gamma_{6,2} = 15$, $\mu_j = 0.2$, $\omega_{j,i} = 0.01$, $k_{1,1} = 25$, $k_{1,2} = 35$, $k_{2,1} = 30$, $k_{2,2} = 25$, $k_{3,1} = 25$, $k_{3,2} = 25$, $k_{4,1} = 20$, $k_{4,2} = 30$, $k_{5,1} = 20$, $k_{5,2} = 20$, $k_{6,1} = 20$, $k_{6,2} = 15$, $\gamma_{\beta_j} = 1$ and $\xi_j = 0.01$.

Figure 1. Communication diagram for all the agents

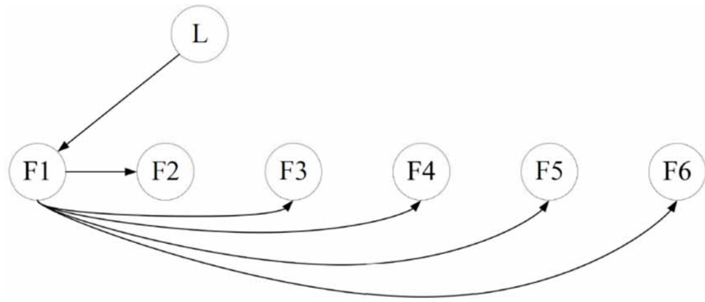

Given the initial value as $x_1(0)=[0.1,-0.2]^T$, $x_2(0)=[0.2,-0.2]^T$, $x_3(0)=[-0.1,0.2]^T$, $z(0)=0.1$, $\hat{\theta}_1(0)=\hat{\theta}_2(0)=\hat{\theta}_3(0)=0.01$, and the other initial conditions are all zero.

Our results are depicted in Figure 2-5. Figure 2 shows the trace curves of the output for six following nodes and one leading node output. Figure 3 shows the consensus tracking error signals. Figure 4 displays the trajectory of the estimation parameters for six followers. The actual dead-zone input and output for all six followers are shown in Figure 5. It can be deduced from all the above results that all the consensus errors uniformly approach a small range around the zero point, and all the adaptive parameters and control signals are bounded. We further conclude that the presented distributed consensus tracking control method is effective and fulfils the control target.

Figure 2. Output tracks of six following nodes

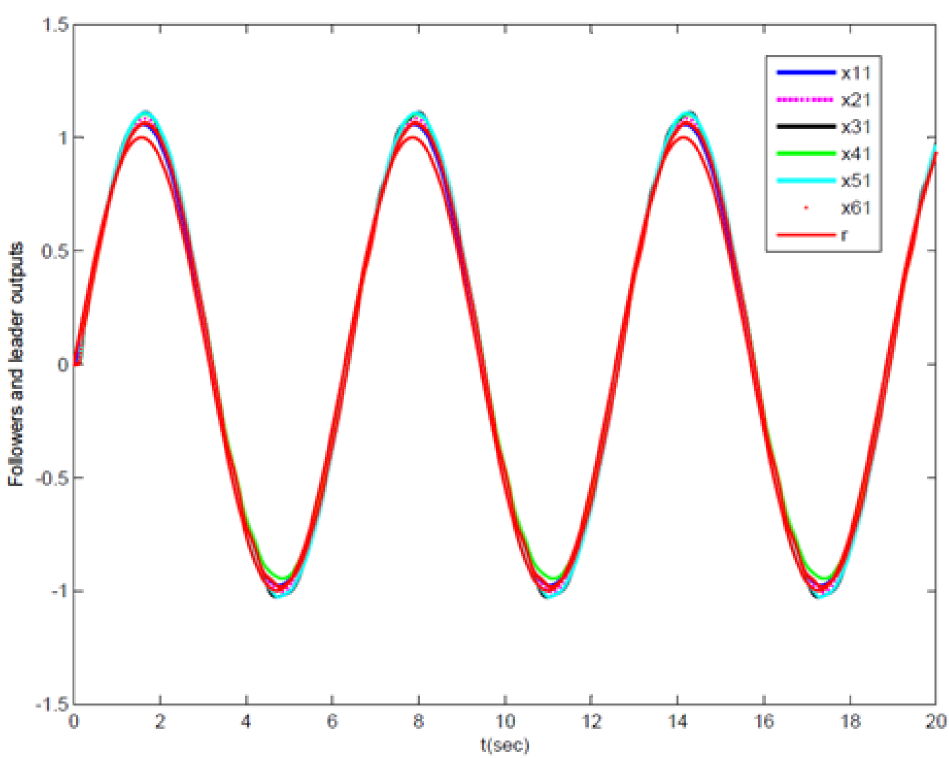

Figure 3. Cooperative tracking error curves

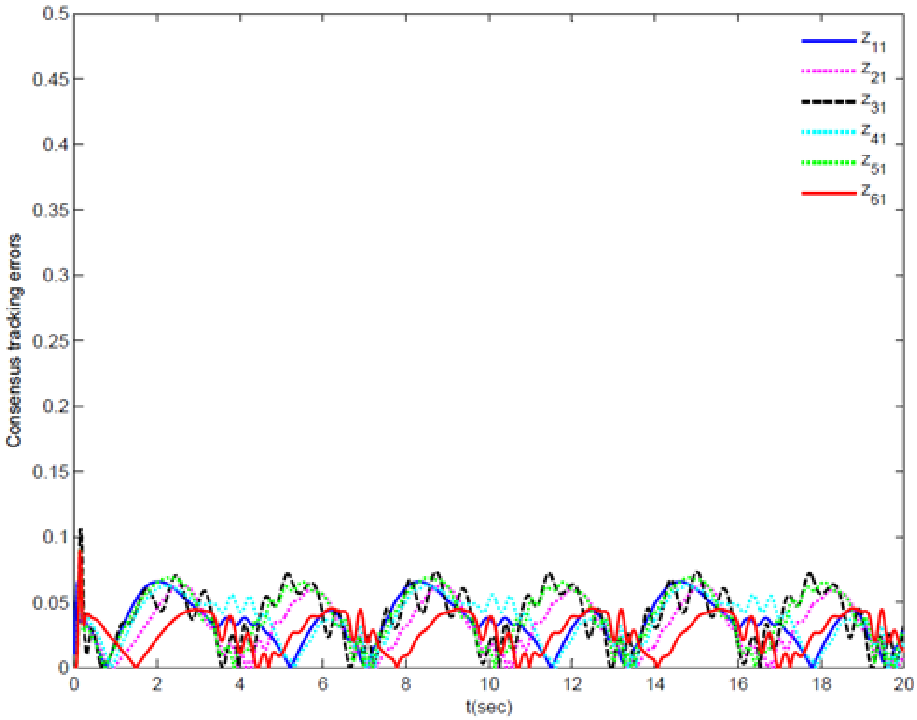

Figure 4. Adaptive parameters $\hat{\theta}_j$ curves

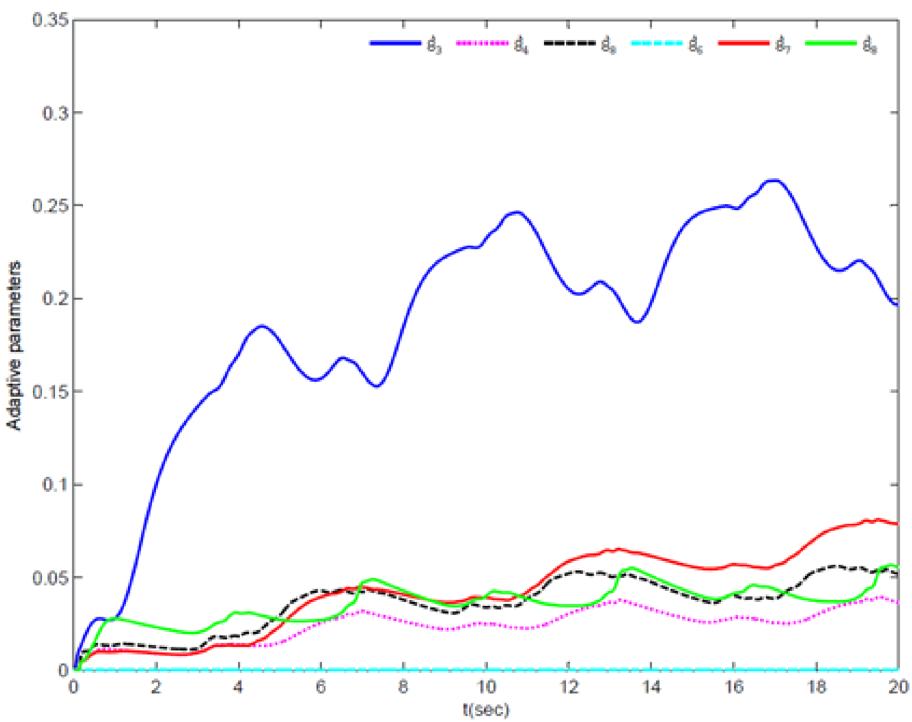

Figure 5. Trajectories of the input signal

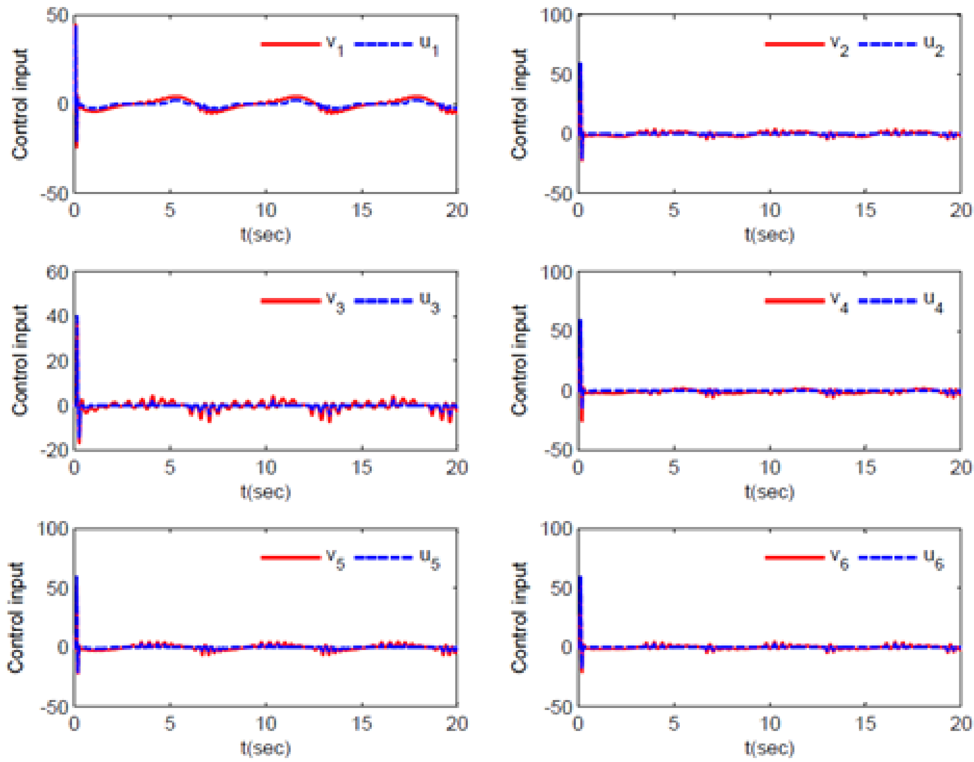

Remark 5.1 Figure 5 displays the curves of v_j and u_j of six followers. v_j represents the dead-zone input of u_j, which is achieved in the last step of the backstepping recursive process. By definition u_j in (2), we can obtain that u_j is a piecewise function of v_j, and it also demonstrates a certain nonsensitivity to small control inputs. Thus, we draw Figure 5 to show the relationship between v_j and u_j.

Without Dead-Zone Input

To verify that our presented control algorithm can reach the same control result even with unknown nonlinear dead-zone input, we carry out a comparison experiment between the proposed controller and the controller in (Jiang, Su & Niu, 2022). The dynamic model is introduced in Section 5.1, which is shared by the two control methods under all the same initial values and parameter selections. All comparison outcomes regarding the consistency error are illustrated in Figure 6. It is concluded that there is little difference in the absolute value of the consensus tracking errors by comparing Figure 3 with Figure 6. In addition, this presented control law is also applicable for more general systems, significantly reducing the number of adoption parameters.

CONCLUSION

In this work, a neuro-based robust adaptive backstepping control method has been developed for high-order MASs with unmodelled dynamics, dynamic disturbances and unknown dead zones. With

Figure 6. Trajectories of cooperative tracking errors without dead-zone input

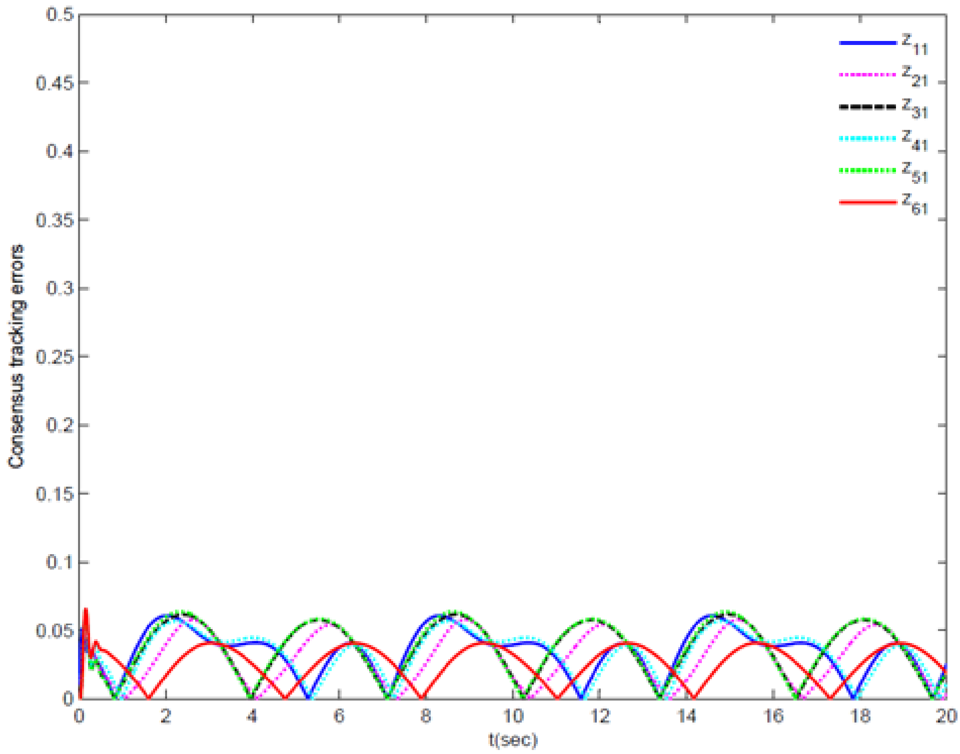

the help of NN approximation, the nonlinear items produced by backstepping recursively for each follower are considered as a whole to be approximated. To handle unmodelled dynamics, an auxiliary dynamic signal is defined to build a proper Lyapunov function. The unknown nonlinear dead-zone input can also be decomposed to an input similar to the perturbed parts. A new inequality is introduced to handle the unknown dead zone. The target tracking errors will be driven to a small region of zero, provided proper design parameters are chosen. The proposed method does not require the dead-zone parameters to be known and only one parameter to be estimated for each follower. In addition, it is robust to unmodelled dynamics and unknown disturbances. However, the consensus errors are associated with the design parameters and some bounded terms of the estimated parameters, and the transient performance needs to be further improved. Future research can focus on developing new control strategies to handle input dead-zone. This includes compensation techniques of dead-zone, input prediction or estimation methods and feedback linearization. The current research mainly focuses on uniform network structure, in the future, we can explore more irregular and complex network, and develop more practical controllers based on these network topologies. Besides, the proposed algorithm can be applied to practical applications and further verified by experiments.

DATA AVAILABILITY

The data used to support the findings of this study are included within the article.

FUNDING STATEMENT

This work was supported by the Open Research Project of the State Key Laboratory of Industrial Control Technology, Zhejiang University, China (No. ICT2023B39).

CONFLICTS OF INTEREST

The authors declare no conflict of interest.

REFERENCES

Aghababa, M. P., & Moradi, S. (2021). Robust adaptive dynamic surface back-stepping tracking control of high-order strict-feedback nonlinear systems via disturbance observer approach. *International Journal of Control*, *94*(9), 2479–2495. doi:10.1080/00207179.2020.1712478

Chang, L., Huang, R., & Park, J. (2020). Robust guaranteed cost control under digital communication channels. *IEEE Transactions on Industrial Informatics*, *16*(1), 319–327. doi:10.1109/TII.2019.2916146

Chang, Y., Zhang, S., Alotaibi, N. D., & Alkhateeb, A. F. (2020). Observer-based adaptive finite-time tracking control for a class of switched nonlinear systems with unmodeled dynamics. *IEEE Access : Practical Innovations, Open Solutions*, *8*, 2479–2495. doi:10.1109/ACCESS.2020.3023726

Chen, T., Yuan, J., & Yang, H. (2022). Event-triggered adaptive neural network backstepping sliding mode control of fractional-order multi-agent systems with input delay. *Journal of Vibration and Control*, *28*(23-24), 3740–3766. doi:10.1177/10775463211036827

Chiang, T., Che, Z., Huang, Y., & Tsai, C. Y. (2022). Using an Ontology-Based Neural Network and DEA to Discover Deficiencies of Hotel Services. *International Journal on Semantic Web and Information Systems*, *18*(1), 1–19. doi:10.4018/IJSWIS.306748

Hammad, M., Alkinani, M. H., Gupta, B., El-Latif, A., & Ahmed, A. (2021). Myocardial infarction detection based on deep neural network on imbalanced data. *Multimedia Systems*, *28*(4), 1373–1385. doi:10.1007/s00530-020-00728-8

Hasib, K., Towhid, N., & Islam, M. (2021). Hsdlm: A hybrid sampling with deep learning method for imbalanced data classification. *International Journal of Cloud Applications and Computing*, *11*(4), 1–13. doi:10.4018/IJCAC.2021100101

He, W., Yan, Z., Sun, Y., Ou, Y., & Sun, C. (2018). Neural-learning-based control for a constrained robotic manipulator with flexible joints. *IEEE Transactions on Neural Networks and Learning Systems*, *29*(12), 5993–6003. doi:10.1109/TNNLS.2018.2803167 PMID:29993842

Hu, G. (2012). Robust consensus tracking of a class of second-order multi-agent dynamic systems. *Systems & Control Letters*, *61*(1), 134–142. doi:10.1016/j.sysconle.2011.10.004

Hua, C., Zhang, L., & Guan, X. (2017). Distributed adaptive neural network output tracking of leader-following high-order stochastic nonlinear multiagent systems with unknown dead-zone input. *IEEE Transactions on Cybernetics*, *47*(1), 177–185. doi:10.1109/TCYB.2015.2509482 PMID:26731786

Huo, X., Ma, L., Zhao, X., & Zong, G. (2020). Event-triggered adaptive fuzzy output feedback control of MIMO switched nonlinear systems with average dwell time. *Applied Mathematics and Computation*, *365*, 1–16. doi:10.1016/j.amc.2019.124665

Jiang, H., Su, W., Niu, B., Wang, H., & Zhang, J. (2022). Adaptive neural consensus tracking control of distributed nonlinear multiagent systems with unmodeled dynamics. *International Journal of Robust and Nonlinear Control*, *32*(16), 8999–9016. doi:10.1002/rnc.6313

Krstic, M., Sun, J., & Kokotovic, P. V. (1996). Robust control of strict and output feedback systems with input unmodeled dynamics. *Proceedings of the 34th Conference on Decision and Control*, *3*, 2257–2262. doi:10.1109/CDC.1995.480539

Li, Y., & Tong, S. (2014). Adaptive fuzzy output-feedback control of pure-feedback uncertain nonlinear systems with unknown dead zone. *IEEE Transactions on Fuzzy Systems*, *22*(5), 1341–1347. doi:10.1109/TFUZZ.2013.2280146

Li, Z., Li, T., & Chen, C. L. (2015). Adaptive NN control for a class of stochastic nonlinear systems with unmodeled dynamics using DSC technique. *Neurocomputing*, *149*, 142–150. doi:10.1016/j.neucom.2013.12.060

Liu, J., Wang, C., & Cai, X. (2021). Adaptive neural network finite-time tracking control for a class of high-order nonlinear multi-agent systems with powers of positive odd rational numbers and prescribed performance. *Neurocomputing*, *419*(4), 157–167. doi:10.1016/j.neucom.2020.08.051

Liu, W., Hu, J., & Li, Y. (2023). Neuro-based adaptive formation control for a class of second-order MASs with unknown state-delays. *IEEE Transactions on Circuits and Wystems. II, Express Briefs*, *70*(6), 2286–2290. doi:10.1109/TCSII.2023.3235060

Nguyen, G., Le Viet, N., Elhoseny, M., Shankar, K., Gupta, B., & Abd El-Latif, A. (2021). Secure blockchain enabled cyber–physical systems in healthcare using deep belief network with Resnet model. *Journal of Parallel and Distributed Computing*, *153*, 150–160. doi:10.1016/j.jpdc.2021.03.011

Pradhan, B., Hussain, M., Srivastava, G., Debbarma, M., Barik, R., & Lin, J. (2022). A neuro-evolutionary approach for software defined wireless network traffic classification. *IET Communications*, ●●●, 1–8. doi:10.1049/cmu2.12548

Qin, Z., He, X., Li, G., & Wu, Y. (2019). Robust adaptive consensus of nonstrict-feedback multi-agent systems with quantized input and unmodeled dynamics. *Information Sciences*, *498*, 117–134. doi:10.1016/j.ins.2019.05.051

Sader, M., Chen, Z., Liu, Z., & Deng, C. (2021). Distributed robust fault-tolerant consensus control for a class of nonlinear multi-agent systems with intermittent communications. *Applied Mathematics and Computation*, *403*, 61–66. doi:10.1016/j.amc.2021.126166

Shahvali, M., & Askari, J. (2022). Distributed adaptive dynamic event-based consensus control for nonlinear uncertain multi-agent systems. *Proceedings of the Institution of Mechanical Engineers. Part I, Journal of Systems and Control Engineering*, *236*(9), 1630–1648. doi:10.1177/09596518221105669

Shen, D., Huo, N., & Saab, S. (2021). A probabilistically quantized learning control framework for networked linear systems. *IEEE Transactions on Neural Networks and Learning Systems*, *33*(12), 7559–7573. doi:10.1109/TNNLS.2021.3085559 PMID:34129506

Shen, Q., & Shi, P. (2016). Output consensus control of multi-agent systems with unknown nonlinear dead-zone. *IEEE Transactions on Systems, Man, and Cybernetics. Systems*, *46*(10), 1329–1337. doi:10.1109/TSMC.2015.2503380

Srivastava, A., Rotte, P., Jain, A., & Prakash, S. (2022). Handling data scarcity through data augmentation in training of deep neural networks for 3D data processing. *International Journal on Semantic Web and Information Systems*, *18*(1), 1–16. doi:10.4018/IJSWIS.297038

Sun, W., Su, S., Wu, Y., & Xia, J. (2020). Novel adaptive fuzzy control for output constrained stochastic nonstrict feedback nonlinear systems. *IEEE Transactions on Fuzzy Systems*, *29*(5), 1188–1197. doi:10.1109/TFUZZ.2020.2969909

Sun, X., & Ge, S. (2022). A DSC approach to adaptive dynamic region-based tracking control for strict-feedback non-linear systems. *IET Control Theory & Applications*, *16*(1), 94–111. doi:10.1049/cth2.12210

Wu, J., Sun, W., Su, S., & Xia, J. (2022). Neural-based adaptive control for nonlinear systems with quantized input and the output constraint. *Applied Mathematics and Computation*, *413*, 1–15. doi:10.1016/j.amc.2021.126637

Xiao, S., & Dong, J. (2021). Cooperative fault-tolerant containment control for nonlinear multiagent systems with switching directed topologies based on hierarchical mechanisms. *IEEE Transactions on Systems, Man, and Cybernetics. Systems*, *52*(9), 5424–5433. doi:10.1109/TSMC.2021.3125772

Yang, H., & Wang, H. (2016). Robust adaptive fault-tolerant control for Uncertain nonlinear system with unmodeled dynamics based on fuzzy approximation. *Neurocomputing*, *173*, 1660–1670. doi:10.1016/j.neucom.2015.09.039

Yang, X., Zhao, W., Yuan, J., Chen, T., Zhang, C., & Wang, L. (2022). Distributed optimization for fractional-order multi-agent systems based on adaptive backstepping dynamic surface control technology. *Fractal and Fractional*, *6*(11), 642–658. doi:10.3390/fractalfract6110642

Yen, S., Moh, M., & Moh, T. (2021). Detecting compromised social network accounts using deep learning for behavior and text analyses. *International Journal of Cloud Applications and Computing*, *11*(2), 97–109. doi:10.4018/IJCAC.2021040106

Zhao, X., Tiao, B., & You, M. (2022). Adaptive distributed sliding mode control for multiple unmanned aerial vehicles with prescribed performance. *IEEE Transactions on Vehicular Technology*, *71*(11), 11480–11490. doi:10.1109/TVT.2022.3192350

Zhao, X., Wang, X., Ma, L., & Zong, G. (2020). Fuzzy-approximation-based asymptotic tracking control for a class of uncertain switched nonlinear systems. *IEEE Transactions on Fuzzy Systems*, *28*(4), 632–644. doi:10.1109/TFUZZ.2019.2912138

Zhu, Q., Liu, Y., & Wen, G. (2020). Adaptive neural network output feedback control for stochastic nonlinear systems with full state constraints. *ISA Transactions*, *101*, 60–68. doi:10.1016/j.isatra.2020.01.021 PMID:32029237

APPENDIX

The global Lyapunov function is selected below:

$$V = \sum_{l=1}^{M} V_{l,s} \tag{A1}$$

From (17), it can be rewritten as follows:

$$\begin{aligned}\dot{\xi}_{l,s+1} &= \Phi_{l,s+1}\left(x_{l,1},\ldots,x_{l,s},x_{i,1},x_{i,2},x_{i,3},y_r,\dot{y}_r,\ddot{y}_r,\hat{\theta}_l\right) \\ &\quad - \frac{\xi_{l,s+1}}{l_{l,s+1}}\end{aligned} \tag{A2}$$

where

$$\begin{aligned}\Phi_{l,s+1}(\cdot) &= -\sum_{i=1}^{k}\frac{\partial \alpha_{l,s}}{\partial x_{j,i}}\dot{x}_{j,i} - \sum_{i=1}^{M}\frac{\partial \alpha_{l,s}}{\partial x_{i,1}}\dot{x}_{i,1} \\ &\quad -\sum_{i=1}^{M}\frac{\partial \alpha_{l,s}}{\partial x_{i,2}}\dot{x}_{i,2} - \frac{\partial \alpha_{l,s}}{\partial y_r}\dot{y}_r - \frac{\partial \alpha_{l,s}}{\partial \hat{\theta}_l}\dot{\hat{\theta}}_l\end{aligned} \tag{A3}$$

where $\Phi_{l,s+1}(\cdot)$ is continuous and bounded with $M_{l,s+1}$.
By differentiating (A1) and using (60), one has

$$\begin{aligned}\dot{V} \le \sum_{l=1}^{M}\Bigg\{&-\sum_{s=1}^{m} k_{l,s}\underline{g}_l z_{l,s}^2 - \frac{\mu_l}{2\gamma_l}\tilde{\theta}_l^2 - \frac{1}{2}m_{l,0}\underline{g}_l\gamma_{\beta_l}\tilde{\beta}_l^2 \\ &+\sum_{s=2}^{m}\xi_{l,s}\dot{\xi}_{l,s} + \sum_{s=1}^{m-1} z_{l,s}g_{l,s}\xi_{l,s+1} + D_{l,m} \\ &+ z_{l,m}g_{l,m}\rho_l(v_l)\Bigg\} - \left(c_0\lambda_0^{-1} - \lambda_0^{-2}\right)r^2\end{aligned} \tag{A4}$$

Applying Young's inequality, we obtain

$$g_{l,s}z_{l,s}\xi_{l,s+1} \le \bar{g}_l^2 z_{l,s}^2 + \frac{1}{4}\xi_{l,s+1}^2 \tag{A5}$$

$$g_{l,m}z_{l,m}\rho_l \le \bar{g}_l^2 z_{l,m}^2 + \frac{1}{4}\rho_l^{*2} \tag{A6}$$

$$\begin{aligned}\xi_{l,s}\dot{\xi}_{l,s} &= -\frac{\xi_{l,s}^2}{l_{l,s}} + \xi_{l,s}\Phi_{l,s}(\cdot) \\ &\le -\frac{\xi_{l,s}^2}{l_{l,s}} + \frac{1}{4\kappa_{l,s}^2}M_{l,s}^2\xi_{l,s}^2 + \kappa_{l,s}^2\end{aligned} \tag{A7}$$

Substituting (A5)-(A7) into (A4), we obtain

$$\dot{V} \le \sum_{l=1}^{M} \left\{ \sum_{s=1}^{m-1} \left(\frac{1}{4} - \frac{1}{l_{l,s+1}} + \frac{M_{l,s+1}^2}{4\kappa_{l,s+1}^2} \right) \xi_{l,s+1}^2 - \frac{\mu_l}{2\gamma_l} \tilde{\theta}_l^2 \right.$$
$$\left. - \sum_{s=1}^{m} \left(k_{l,s} \underline{g}_l - \bar{g}_l^2 \right) z_{l,s}^2 - \frac{1}{2} m_{l,0} \underline{g}_l \gamma_{\beta_l} \tilde{\beta}_l^2 \right\} \tag{A8}$$
$$- \left(c_0 \lambda_0^{-1} - \lambda_0^{-2} \right) r^2 + \sum_{l=1}^{M} D_{l,m} + \sum_{l=1}^{M} \sum_{s=1}^{m-1} \kappa_{l,s+1}^2$$
$$+ \frac{1}{2} \sum_{l=1}^{M} \frac{\mu_l}{\gamma_l} \theta_l^2 + \frac{1}{2} \sum_{l=1}^{M} m_{l,0} \underline{g}_l \gamma_{\beta_l} \beta_l^2$$

Now, by defining the parameters $k_{l,s}^0$, $m_{l,s}^0$, $l = 1,2,\cdots,M$, and $s = 1,2,\cdots,m$ as follows:

$$k_{l,s}^0 = k_{l,s} \underline{g}_l - \bar{g}_l^2, \; m_{l,s}^0 = \frac{1}{l_{l,s+1}} - \frac{1}{4} - \frac{M^2}{4\beta_{l,s+1}^2}$$

we have

$$\dot{V} \le -C_1 V + C_2 \tag{A9}$$

where

$$C_1 = \min\left\{ 2k_{l,s}^0, 2m_{l,s}^0, 2\left(c_0 - \lambda_0^{-1}\right), \mu_l, \gamma_{\beta_l} \right\}, C_2 = \sum_{l=1}^{M} \left(D_{l,m} + \sum_{s=1}^{m-1} \kappa_{l,s+1}^2 + \frac{1}{2} \frac{\mu_l}{\gamma_l} \theta_l^2 + \frac{1}{2} m_{l,0} \underline{g}_l \gamma_{\beta_l} \beta_l^2 \right)$$

Using the integral over (A9) on [0,T], the following inequality is obtained:

$$0 \le V(T) \le \left(1 - e^{-C_1 T}\right) \frac{C_2}{C_1} + V(0) e^{-C_1 T} \le V(0) + \frac{C_2}{C_1} \tag{A10}$$

Let $\Xi = V(0) + \dfrac{C_2}{C_1}$, we can easily obtain that as $t \to \infty$, $\left\| z_{l,s} \right\| \le \sqrt{2\Xi}$.
Moreover, by the definition of the expression of V in (A1), the bounds of all closed-loop signals are obviously guaranteed.